Journal of
Marine Science and Engineering

MDPI

Article

R&D of an Innovative OFDM Communication Payload for Small-Size AUV

Bin Li [1], Feng Tong [2,3,4,*], Xiujing Gao [1], Junhui Yao [2,4], Yuehai Zhou [2,3] and Hongwu Huang [1]

1 Institute of Smart Marine and Engineering, Fujian University of Technology, Fuzhou 350118, China; libin@fjut.edu.cn (B.L.); gaoxiujing@fjut.edu.cn (X.G.); huanghongwu@fjut.edu.cn (H.H.)
2 College of Ocean and Earth Sciences, Xiamen University, Xiamen 361002, China; 22320211151407@stu.xmu.edu.cn (J.Y.); zhouyuehai@xmu.edu.cn (Y.Z.)
3 National and Local Joint Engineering Research Center for Navigation and Location Service Technology, Xiamen University, Xiamen 361002, China
4 Institute of Artificial Intelligence, Xiamen University, Xiamen 361002, China
* Correspondence: ftong@xmu.edu.cn

Abstract: With its superiorities of low cost, high flexibility and deployment convenience, small-size autonomous underwater vehicles (AUVs) have been extensively applied to perform a variety of undersea missions. While underwater acoustic (UWA) communication provides a practical way to establish a wireless link, it still poses a significant challenge due to the strict limitations of a small-size AUV platform in terms of load capacity, energy supply and cost. Orthogonal frequency division multiplexing (OFDM) has drawn extensive attention due to its high data rate capability and relative robustness to multipath, the performance of which is unfortunately sensitive to the widespread Doppler effect. While efficient Doppler compensation is significantly crucial for UWA OFDM mobile communication, most of the conventional approaches are conducted using software resampling, thus rendering a huge burden on memory and calculation capability as well as a considerable processing delay. In this paper, from the perspective of hardware completion an UWA OFDM communication payload based on STM32F407 processor is designed and implemented to facilitate agile Doppler compensation with low computational overhead. In particular, after estimating Doppler by calculating the time compression or extension of the preamble signal, Doppler compensation is performed by directly adjusting the direct digital frequency synthesizer (DDS)-driven sampling rate of the analog-to-digital converter (ADC). As the Doppler is compensated parallel to the ADC acquisition, processing delay and memory requirement can be avoided. Finally, hardware-in-loop (HIP) simulation is performed to demonstrate the effectiveness and superiority of the proposed system. The results show that the designed system has the potential to achieve an effective communication rate of 3.19 kbps with the admissible implementation overhead. Future work will entail the integration and performance evaluation of the proposed UWA OFDM communication payload on a practical small-size AUV platform.

Keywords: Doppler compensation; orthogonal frequency division multiplexing (OFDM); direct digital frequency synthesizers (DDS); underwater acoustic (UWA) communication

Citation: Li, B.; Tong, F.; Gao, X.; Yao, J.; Zhou, Y.; Huang, H. R&D of an Innovative OFDM Communication Payload for Small-Size AUV. *J. Mar. Sci. Eng.* **2023**, *11*, 1029. https://doi.org/10.3390/jmse11051029

Academic Editor: Rouseff Daniel

Received: 16 April 2023
Revised: 6 May 2023
Accepted: 10 May 2023
Published: 12 May 2023

1. Introduction

With the dramatically increasing requirement for ocean information perception and acquisition, autonomous underwater vehicle (AUV) play an increasingly important role in not only the traditional field of marine resource exploration, hydrological environment investigation, seabed topographic mapping or reconstruction [1,2], but also emerging personal applications such as underwater sightseeing, swimming aid and entertainment purposes [3]. In particular, as an important branch of AUV development, in recent years, small-size AUV platforms have drawn extensive attention due to their low cost, small size and high flexibility characteristics.

Consider the serious limitation of load capacity, energy supply and cost posed by a small-size AUV platform, it has become an urgent problem to establish as efficient underwater wireless communication link between small-size AUV platforms and the control mother ship. With its easy availability of existing commercial products, many small-size AUVs employ radio or optical communication modules for achieving information transmission near the water surface. However, this type of small-size AUV is extremely limited by the essential constraints in the aspect of communication distance and stability.

Underwater acoustic (UWA) communication technology offers a feasible approach to accomplish the underwater requirements of small-size AUV in terms of underwater telemetry, remote control and data transmission [4]. However, the intertwined properties of marine environment contained tide, wave, current and interfacial effect generate the adverse UWA channel characteristics such as complicated multipath, dynamic Doppler, fast time-varying, severe fading and background noise, which can pose a significant challenge to the UWA communication system onboard small-size AUV [5,6].

Moreover, the incoherent communication technology cannot meet the demands of high-speed data rate for the multitudinous applications of small-size AUV in marine data acquisition and transmission with its constraints of low bandwidth utilization in the severely constrained UWA channels [7]. Different to the incoherent mode, coherent communication provides an effective approach to clearly improve the data transmission rate. However, the phase variations of modulated UWA signals caused by the complicated time-space-frequency characteristics of UWA channel lead to a serious impact on the communication performance. Among the efforts for this purpose, the technology of orthogonal frequency division multiplexing (OFDM) has gained significant interest because of its promising features of a high data transmission rate, high spectrum efficiency and strong anti-multipath [8,9].

Nonetheless, the performance of OFDM is sensitive to Doppler effect generated by the time-varying UWA channel or moving AUV [10], which generates the accumulation of symbol synchronization error and the destruction of orthogonality and seriously deteriorates the demodulation performance of the receiver. Thus, Doppler estimation and compensation are essential steps in the research and development (R&D) of UWA OFDM communication for realizing stable UWA OFDM communication performance. Numerous Doppler estimation and compensation approaches have been extensively reported.

A typical strategy is to estimate Doppler by measuring the frequency offset of the single-frequency signal with known frequency between the received packets and the transmitted signal [11]. Nevertheless, the estimation accuracy of such algorithms with the classic fast Fourier transform (FFT) is insufficient due to its spectrum leakage of windowed signal after FFT calculation. With the purpose of improving the estimation accuracy, some novel approaches such as fractional Fourier transform (FRFT) [12], partial fast Fourier transform (PFFT) [13] and partially shifted fast Fourier transform [14] are introduced to replace the classic FFT with respect to the based frequency measurement Doppler estimation methods. However, this type of algorithms causes severe performance degradation while the estimated signal passes the frequency-selective fading channel.

The classic cross-correlation estimation schemes realize extremely high-precision Doppler estimation in complex underwater multipath channel with calculating cross-ambiguity function (CAF) between transmitted and received packets [15,16]. However, as the maximum CAF magnitude calculation is accomplished utilizing enormous searches in a two-dimensional grid of Doppler factors and delays, tremendous amounts of searching grids cause intensive computational complexity. In order to overcome the interference of enormous calculations, the stepwise cross-correlation estimation strategies (coarse estimation and fine estimation) were proposed and investigated, which can effectively reduce the number of searching grids and accelerate computation [17].

The single-branch auto-correlation (SBA) strategies have been extensively inquired to estimate Doppler factor through calculating the period variation of the periodical transmitted signal [18,19]. However, the SBA approaches cannot be applied to scenarios where there is acceleration. With the purpose of expanding the applicability of the SBA methods, a multi-branch auto-correlation (MBA) algorithm [20] was proposed and investigated to address fast-moving and manoeuvring vehicles, the performance of which is comparable to that of the classic cross-correlation estimation schemes.

An ultra-precision Doppler estimation strategy based on the minimum bit error rate (BER) principle was proposed and investigated to transform the signal-level Doppler estimation into the bit-level search [21]. With the purpose to restrain the massive BER searching, an iterative BER gradient descent algorithm [22] was investigated to accomplish the same estimation accuracy with the BER search strategy revealed in [21]. Nevertheless, this type of Doppler estimation strategy based on BER information requires the inclusion of a demodulation process in the process of Doppler estimation.

Note that, while many more different types of investigations in Doppler estimation have been conducted, most of the previous work adopted resampling for Doppler compensation. In other words, after obtaining the Doppler factor via different types of estimation methods, Doppler compensation is generally realized by interpolation resampling in time domains according to the Doppler factor [23].

However, while it is relatively convenient to perform resampling using the software, considerable processing delays will be unavoidably generated. Thus, the agility of Doppler compensation poses a challenge for the design of the UWA OFDM system for AUV with agile moving capability or under rapidly time-varying UWA channels. With the purpose of enabling agile Doppler compensation, a hardware resampling scheme was designed to enable resampling via an adjustable sampling rate analog-to-digital Converter (ADC), which is driven by a precision-limited processor clock [24].

In this paper, by further improving the hardware resampling accuracy, a novel UWA OFDM communication payload based on STM32F407 processor is designed and implemented to facilitate agile Doppler compensation at the expense of low computational overhead. Specially, the proposed payload adopted a classic time-frequency OFDM receiver structure [25] with respect to simple implementation and low complexity onboard small-size AUV. Doppler estimation was accomplished with the classic method described in [23]. For agile and low computational overhead Doppler compensation, Direct Digital Frequency synthesizers (DDS) chip AD9954 controlled by STM32F407 processor is adopted to generate adjustable sampling clock frequency for ADC. The validity and superiority of the proposed scheme are verified through hardware-in-loop (HIP) simulation on the UWA OFDM modem that can be mounted properly on a small-size AUV platform.

The rest of this paper is organized as follows. In Section 2, the detailed signal model, time-frequency differential OFDM coding, Doppler estimation and compensation implementation are introduced. Section 3 describes the HIP simulation results to verify the performance of the proposed UWA communication payload. In Section 4, we introduce accuracy and availability analysis for the proposed scheme. Conclusions are summarized in Section 5.

2. Systems and Methods

2.1. Basic Signal Model

Without loss of generality, one cyclic-prefixed (CP) OFDM block can be formulated as

$$s(t) = \Re\left\{ e^{j2\pi f_c t} \sum_{k=-L/2}^{L/2-1} s[k] e^{j2\pi \frac{k}{T_s} t} g(t) \right\}, \tag{1}$$

where f_c is the center frequency, $s[k]$ denotes the symbol to be transmitted on the k-th sub-carrier, and T_s is the basic OFDM symbol duration. Let L represent the number of sub-carriers, which dictates that the k-th sub-carrier is located at the frequency

$$f_k = \frac{k}{T_s},\ k = -\frac{L}{2}, -\frac{L}{2}+1, \ldots, \frac{L}{2}-1, \tag{2}$$

Let T_{cp} denote the length of the CP, and $g(t)$ can be defined as a rectangular window of length $T_{cp} + T_s$

$$g(t) = \begin{cases} 1, t \in [-T_{cp}, T_s] \\ 0, \text{otherwise} \end{cases}, \tag{3}$$

One can assume that the UWA channel can be modeled as a time-varying linear system, and the Doppler effect on each path is uniform. Letting the p-th amplitude response maintain constant over one OFDM block, the UWA channel response can be expressed as

$$h(t,\tau) = \sum_{p=1}^{N_p} A_p \delta(\tau - \tau_p + \varepsilon t), \tag{4}$$

where N_p is the maximum discernible number of multipath, ε denotes a common Doppler factor, moreover, A_p and τ_p represent the time-varying amplitude response and delay of the p-th path, respectively.

Based on the previous assumptions, letting the CP-OFDM signal pass through the channel as described in (4), the received baseband signal can be formulated as

$$r(t) = \sum_{k=-L/2}^{L/2-1} \left\{ s[k] e^{j2\pi f_k t} e^{j2\pi \varepsilon f_k t} \left[\sum_{p=1}^{N_p} A_p e^{-j2\pi f_k \tau_p} \right] g(t + \varepsilon t - \tau_p) \right\} + n(t), \tag{5}$$

where $n(t)$ is the baseband white Gaussian noise. Note that the Doppler effects on received OFDM packets can be expressed as

$$\xi_k = e^{j2\pi k \varepsilon f_k t}. \tag{6}$$

Based on the above derivation, Doppler estimation and compensation are essential to eliminate the interference of (6) for accomplishing robust mobile UWA OFDM communication.

2.2. Time-Frequency Differential OFDM Scheme

The common time-frequency differential OFDM scheme with strong anti-multipath ability and good channel adaptability is applied to the proposed UWA communication payload. The time-domain differential modulation is completed at adjacent OFDM symbols, and then the data information and its inverse data are loaded into the adjacent subcarriers to accomplish the frequency-domain modulation. The signal model of the above scheme is introduced briefly as follows.

Assuming that the data on the n-th subcarrier of the i-th OFDM symbol before differential modulation can be written as

$$D_{i,n} = e^{j\phi_{i,n}}, \tag{7}$$

where $\phi_{i,n} 0, 2\pi$ denotes the phase of the n-th subcarrier of the i-th OFDM symbol, $n = \left(0, 2, \ldots, 2\left(\frac{L}{2} - 1\right)\right)$ is the index of data subcarrier. The data after differential modulation can be expressed as

$$S_{i,n} = e^{j\Delta\phi_{i,n}}, \tag{8}$$

Hence, the phase information at the same index subcarriers on the adjacent OFDM symbols can be formulated as

$$\Delta\phi_{i,n} = \phi_{i,n} + \Delta\phi_{i-1,n}, \tag{9}$$

Furthermore, the phase information at the adjacent index subcarriers on the same OFDM symbol can be written as

$$\Delta\phi_{i,n+1} = -(\phi_{i,n} + \Delta\phi_{i-1,n}), \tag{10}$$

As a consequence, the phase in (9) is loaded into (n + 1)-th subcarrier as the pilot symbol

$$S_{i,n+1} = e^{j\Delta\phi_{i,n+1}} = e^{-j\Delta\phi_{i,n}}. \tag{11}$$

At the receiving end, the data of the n-th and (n + 1)-th of the i-th OFDM symbol can be formulated as

$$R_{i,n} = A_{i,n}H_{i,n}e^{j\phi_{i,n}(\varepsilon)} + n_{i,n} = A_{i,n}H_{i,n}e^{j(\Delta\phi_{i,n}+\theta_{i,n}(\varepsilon))} + n_{i,n}, \tag{12}$$

$$R_{i,n+1} = A_{i,n+1}H_{i,n+1}e^{j\phi_{i,n+1}(\varepsilon)} + n_{i,n+1} = A_{i,n+1}H_{i,n+1}e^{j(\Delta\phi_{i,n+1}+\theta_{i,n+1}(\varepsilon))} + n_{i,n+1}, \tag{13}$$

where $A_{i,n}$ and $A_{i,n+1}$ denote the amplitude factor, $H_{i,n}$ and $H_{i,n+1}$ represent the channel impulse response, $\theta_{i,n}$ and $\theta_{i,n+1}$ are the phase deviation, and $n_{i,n}$ and $n_{i,n+1}$ denote the white Gaussian noise.

The phase information in (12) and (13) is extracted to perform the differential demodulation, the demodulation results are presented as follows:

$$\hat{\phi}_{i,n}(\varepsilon) = (\Delta\phi_{i,n} + \theta_{i,n}(\varepsilon)) - (\Delta\phi_{i-1,n} + \theta_{i-1,n}(\varepsilon)) = \phi_{i,n} + (\theta_{i,n}(\varepsilon) - \theta_{i-1,n}(\varepsilon)), \tag{14}$$

$$\hat{\phi}_{i,n+1}(\varepsilon) = (\Delta\phi_{i-1,n+1} + \theta_{i-1,n+1}(\varepsilon)) - (\Delta\phi_{i,n+1} + \theta_{i,n+1}(\varepsilon)) = \phi_{i,n} + (\theta_{i-1,n+1}(\varepsilon) - \theta_{i,n+1}(\varepsilon)), \tag{15}$$

Thus, the data symbols are corrected by the pilot symbols to recover the phase information on the n-th subcarrier of the i-th OFDM symbol

$$\overline{\phi}_{i,n}(\varepsilon) = \frac{\hat{\phi}_{i,n}(\varepsilon) + \hat{\phi}_{i,n+1}(\varepsilon)}{2} = \phi_{i,n} + \Delta\theta(\varepsilon), \tag{16}$$

where $\Delta\theta$ is the phase bias introduced by the complicated characteristic of an UWA channel. According to the above derivation, the initial phase information can be recovered utilizing the differential detection.

In conclusion, there is no requirement for channel estimation and compensation by employing the above time-frequency differential OFDM scheme to eliminate the interference of Doppler effect on UWA OFDM communication, further facilitating the low complexity design and implementation of an UWA OFDM communication payload for small-size AUV platforms.

2.3. Doppler Estimation and Compensation Implementation

In this section, an UWA OFDM payload is designed and investigated to enable agile Doppler compensation with low computational overhead. Before the Doppler compensation, Doppler estimation is achieved by adopting the modified signal frame structure shown in Figure 1; in particular, the Doppler factor can be estimated by calculating the time compression or extension of the received preamble signal after the synchronization is achieved [23].

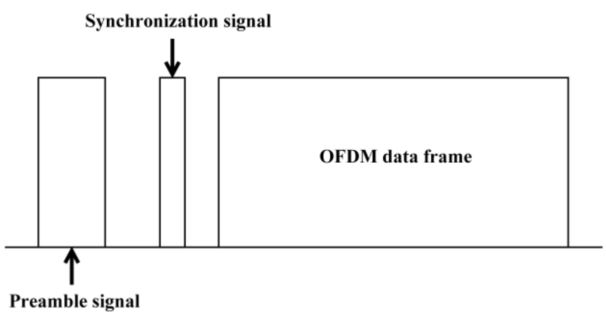

Figure 1. The structure of the signal frame.

2.3.1. Doppler Estimation Strategy

Considering the Doppler effects on the received OFDM packets, the received signal can be rewritten as

$$r(t) = s((1+\varepsilon)t), \tag{17}$$

If T_{sam} represents the sampling period, the discrete received version of $r(t)$ can be formulated as

$$r(n) = s((1+\varepsilon)kT_{sam}), \tag{18}$$

As the Doppler spread is equivalent to the contraction or expansion of the received OFDM packet in time domain, herein the time amount variation of the preamble sequence containing ten linear frequency modulation (LFM) signals is transformed into the Doppler factor as follows:

$$\varepsilon = \frac{L_r - L_t}{L_t}. \tag{19}$$

where L_r and L_t are the length of the received and the transmitted preamble signal at the time domain, respectively. After Doppler estimation is accomplished, the Doppler compensation is carried out to facilitate the demodulation of the OFDM data frame.

2.3.2. Conventional Doppler Compensation Method

After obtaining the Doppler factor, the conventional Doppler compensation approach is to resample the received data frame packets with linear interpolation for accomplishing Doppler compensation. The implementation process of Doppler compensation is as follows.

First, $r(n)$ is processed by upsampling at M times the original sampling rate; then, the received sequence can be rewritten as

$$r(m) = \sum_{n=-\infty}^{L_n} r(n)h(m - nM), \tag{20}$$

where $h(m) = sinc(m/M)$, and L_n represents the length of $r(n)$. Second, the sampling rate of $r(m)$ is downsampled to $\frac{1}{N}$ times of the sampling rate of $r(n)$ after the upsampling process is completed; accordingly, the received sequence can be formulated as

$$\hat{r}(m) = \sum_{n=-\infty}^{L_n} r(n)h(mN - nM). \tag{21}$$

where $h(m) = \mathrm{sinc}[m/\max(M,N)]$. Accordingly, the Doppler compensation can be accomplished through the above variable sampling process. The implementation of this compensation process on the hardware platform requires two sampling processes on the received signal, which imposes a huge burden on the calculation capacity, memory space and processing delay of the central processing unit (CPU).

2.3.3. Agile and Low Computational Overhead Doppler Compensation Approach

Especially for small-size AUV platforms, the high calculation and storage requirements on CPU result in expensive system costs, which is not conductive to the small-size AUV applications. To address the above limitations, an UWA OFDM payload is designed to enable agile Doppler compensation with low computational overhead. The payload adopts AD9954 chip to generate the control signal of clock frequency, then the sampling rate at the ADC process can be regulated in real time through adjusting the clock frequency of the external clock source of Inter-IC Sound (I2S) bus. The Doppler compensation is accomplished while the acquisition of data segment is performed.

The transmission and reception of signal sequence are realized by a UWA OFDM modem with the architecture presented in Figure 2. The hardware module of the UWA OFDM system mainly consists of STM32F407 processor, signal processing circuit as well as power management unit. Note that, the STM32F407 chip as a core processor with a 32-bit ARM Cortex-M4 core is used exclusively to control timers for data acquisition and processing.

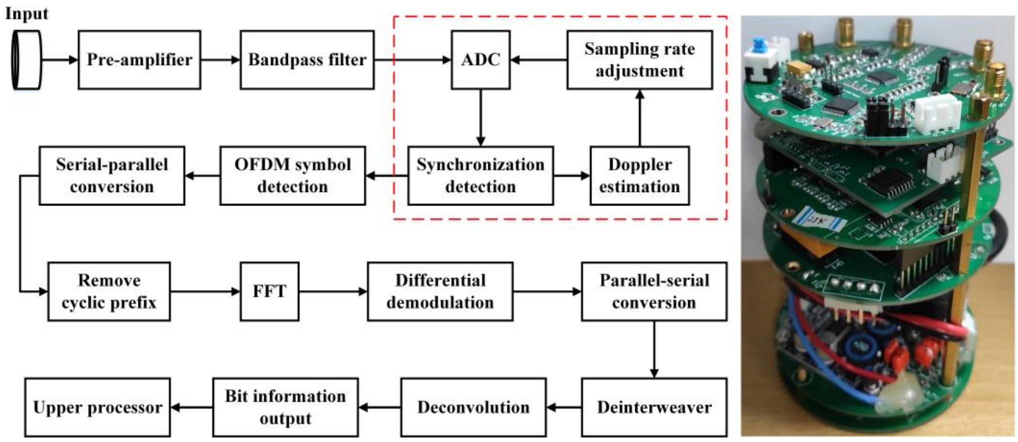

Figure 2. The block chart of the OFDM receiver.

In the process of signal acquisition, the CPU drives the audio acquisition chip WM8978 through the I2S bus interface to perform the ADC process of received signal. The selection of the external clock as the $I2S\_CLK$ clock source provides the feasibility for the real-time adjustment of the sampling rate. The sampling rate for the ADC acquisition process can be expressed as

$$F_s = \frac{I2S\_CLK}{2 \cdot W_f \cdot (2 \cdot I2SDIV + ODD) \cdot 8}, \tag{22}$$

where $I2S\_CLK$ is the clock frequency of the external clock, W_f denotes the frame width of the channel and $I2SDIV$ denotes the value of the I2S linear prescaler with the range of [2 255]. ODD is the odd factor for the linear prescaler, and its value is 0 or 1. As described in (22), the adjustable sampling rates can be acquired through the different combinations of $I2S\_CLK$, $I2SDIV$ and ODD. In conclusion, the core of the sampling rate adjustment can be converted into generating an external clock control signal.

The highly integrated DDS chip AD9954 is felicitously used as a programmable clock generator to produce an external clock control signal due to its ability to generate up to 200 MHz analog sine wave, fast frequency conversion and high frequency resolution through inputting control words in the serial I/O port. The frequency of the AD9954 output signal can be expressed as

$$F_o = \begin{cases} FTW \cdot F_{sys}/2^{32}, & 0 \le FTW \le 2^{31} \\ F_{sys} \cdot \left(1 - \left(FTW/2^{32}\right)\right), & 2^{31} < FTW < 2^{32} - 1 \end{cases}. \tag{23}$$

where F_{sys} is the system clock, FTW is the frequency conversion bytes, and 2^{32} denotes the capacity of the accumulator.

In the processing of signal reception, firstly, the pre-amplifier and bandpass filter are adopted to complete the functions of amplification, filtering and denoising for the received OFDM packets. Secondly, the CPU applies the Doppler factor to calculate the required sampling rate with respect to Doppler correction, further obtains the frequency of external clock control signal according to the (22). Afterwards, the CPU drives the AD9954 chip to generate the clock control signal with corresponding frequency through inputting control words into the serial I/O port; the Doppler compensation is completed synchronously in the acquisition process of the received signal. Thirdly, after acquisition of the OFDM symbol, the CP that can resist the inter symbol interference is removed in order to facilitate the OFDM symbol demodulation. Fourthly, FFT operation is carried out to accomplish the transformation from the time domain signal to the frequency domain signal, and then the mapped sequences located at the corresponding frequency band of OFDM symbol are isolated for differential quadrature phase shift keying (DQPSK) demodulation. Finally, the demodulated binary information is decoded by convolutional decoding and interleaving decoding to recover the transmitted data information.

3. Results

In this section, HIP simulation is performed to evaluate the performance of the proposed UWA OFDM payload onboard small-size AUV platform. The frame structure of transmitted packet is identical to Figure 1, the parameters of which are provided in Table 1. Note that the (2,1,7) convolutional coding with an interleaving depth of 7 is adopted to further improve the communication performance, corresponding to the original communication rate and effective communication rate shown in Table 1.

Table 1. Parameters of transmitted packet.

Items	Value	Items	Value
Modulation mode	DQPSK	OFDM symbol duration (ms)	42.67
Center frequency (Hz)	25,000	Length of guard interval (ms)	10.67
Bandwidth (Hz)	8000	Length of LFM signal (ms)	17.71
Sampling rate (Hz)	96,000	FFT points	4096
Number of sub-carriers	340	Number of OFDM symbol	40
Interval of sub-carrier (Hz)	23.44	Original communication rate (kbps)	6.38
Length of OFDM data frame (ms)	2133.33	Effective communication rate(kbps)	3.19

While the preamble sequence containing ten linear frequency modulation (LFM) signals is inserted before the entire signal frame for preliminary synchronization and Doppler estimation, one LFM signal is located at the beginning of the OFDM data frame for fine timing synchronization to facilitate the demodulation process of OFDM symbols. The setup parameters of LFM signal are consistent with the OFDM data frame.

An artificial UWA channel [26] is generated for HIP simulation, which consists of direct path, surface reflected path and surface-bottom-surface reflected path. The corresponding dominant coefficients are set as the magnitude of 0.76, 0.53 and 0.37, respectively. The other coefficients are set to zero to generate the channel impulse response as displayed in Figure 3. The total multipath delay spread is 10 ms, which is consistent with the scale of some field experimental scenes.

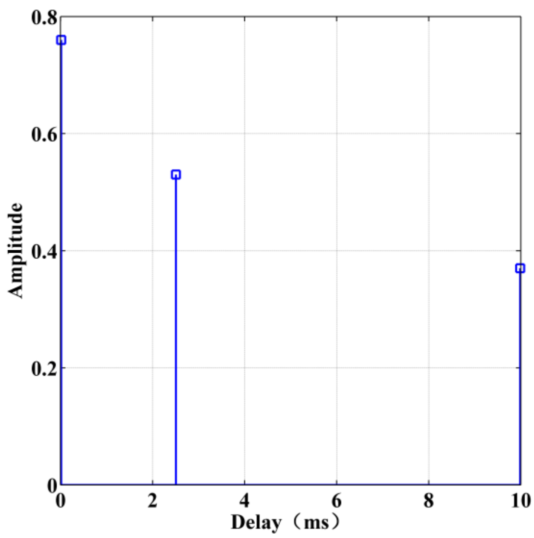

Figure 3. The channel impulse response of simulation channel.

The signal-to-noise rate (SNR) of 0 dB to 20 dB is generated by mixing the additive white Gaussian noise with the signal at an interval of 5 dB. Furthermore, three typical working scenarios of small-size AUV platform including unpowered drifting with seawater, low-speed motion and high-speed motion are employed to verify the Doppler compensation performance of the proposed UWA OFDM payload, corresponding to three Doppler scales of 10 Hz, 25 Hz and 40 Hz introduced by artificial resampling.

The classic time-frequency differential OFDM receiver with the block chart as shown in Figure 2 is adopted for acquisition, Doppler estimation, Doppler compensation and demodulation of the received packets. The results of Doppler estimation and demodulation BER as shown in Figure 4 are used as the fundamental basis to evaluate the feasibility and effectiveness of the designed UWA OFDM payload. The BER is defined as the number of the received error bits divided by the total number of received bits.

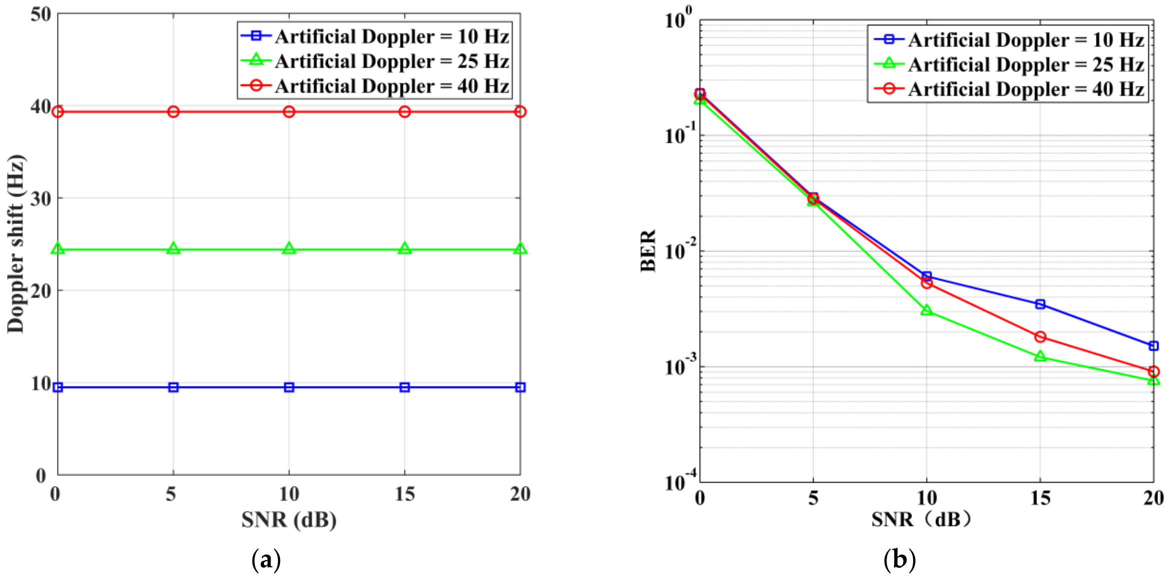

Figure 4. Doppler and BER with respect to SNR. (**a**) Doppler curve over SNR; (**b**) BER curve over SNR.

The Doppler estimation results under different SNR conditions are provided in Figure 4a, from which we can notice that the three scales Doppler curves are independent with respect to different SNRs. While the Doppler scales introduced by artificial resampling are 10 Hz, 25 Hz and 40 Hz, the evaluated Doppler values are 9.49 Hz, 24.41 Hz and 39.33 Hz due to the limitations of estimation accuracy corresponding the Doppler estimation biases of 5.1%, 2.36% and 1.68%, which indicates that the Doppler estimation approach possesses definite robustness.

As revealed in Figure 4b, BER curves of the three Doppler scales tend to decrease with the increase in SNR. Under low SNR conditions, the BER curves are close for the three Doppler scales. When the SNR is greater than 10 dB, the BER results with three Doppler scales are reduced to the order of 10^{-3}, which demonstrates the feasibility and effectiveness of the designed UWA OFDM payload.

4. Discussion

The accuracy and availability of the proposed UWA OFDM communication payload are analyzed in this section. Initially, the Doppler estimation resolution proposed in this paper can be expressed as

$$\Delta\sigma = \frac{1}{(n_{LFM} - 1) \cdot L_s} \cdot f_c, \tag{24}$$

where n_{LFM} is the number of LFM signal contained in the preamble sequence, and L_s represents the total length of one LFM signal and one blank interval. The Doppler estimation bias can be formulated as

$$\begin{aligned} \eta &= |\varepsilon - \varepsilon_d| \cdot f_c \\ &\leq \tfrac{1}{2}\Delta\sigma. \end{aligned} \tag{25}$$

where ε_d is the desired Doppler factor. From (24) we can notice that the Doppler estimation resolution depends on the length of preamble signal. In this paper, let $n_{LFM} = 10$ and $L_s = 2048$, the Doppler estimation resolution is $\Delta\sigma \approx 1.36$ Hz with respect to $\eta \leq 0.68$ Hz. In addition, due to the suppression ability of the time-frequency differential OFDM receiver on small-scale Doppler expansion, the interference of residual Doppler η can be effectively eliminated by differential detection to facilitate OFDM symbol demodulation.

Furthermore, using $I2SDIV = 2$ and $ODD = 0$ in the actual acquisition process, the required adjustable external clock frequency is less than 100 MHz; thus, the AD9954 chip can satisfy the adjustable frequency requirements of clock control signal due to its ability of generating up to 200 MHz analog sine wave. In addition, the frequency resolution of the clock control signal generated by AD9954 chip is 1 Hz, corresponding to the adjustable sampling rate resolution of about 0.001 Hz, and it can also meet the accuracy requirement of signal acquisition with an adjustable audio sampling rate.

5. Conclusions

With the interference of the Doppler effect in the UWA channels, the performance of an UWA OFDM communication system will be seriously degraded. In particular, for an UWA OFDM communication payload onboard small-size AUV, the serious limitations of load capacity, energy supply and cost pose significant challenges.

In this paper, a novel UWA OFDM payload is designed and investigated for a small-size AUV by employing hardware implementation to enable agile Doppler compensation with low computational overhead. After Doppler estimation is completed by calculating the time compression or extension of preamble signal, the DDS chip AD9954 is adopted to enable hardware tuning of the ADC sampling rate via the external clock source of the I2S bus. As the Doppler compensation is fulfilled at the hardware level, any processing delay generated during the software resampling is avoided.

Finally, HIP simulation on the UWA OFDM modem was conducted to demonstrate the effectiveness and superiority of the proposed scheme, with the potential of achieving an effective communication rate of 3.19 kbps with the admissible implementation overhead. The designed and implemented UWA OFDM communication payload has the potential of being applied to small-size AUV platform in multitudinous underwater missions associated with telemetry and remote control between underwater vehicles. Future work will contain the integration and performance evaluation of the proposed UWA OFDM communication payload on the practical small-size AUV platform.

Author Contributions: Conceptualization, B.L. and F.T.; methodology, B.L. and Y.Z.; software, B.L.; validation, Y.Z., J.Y. and B.L.; formal analysis, X.G. and H.H.; investigation, J.Y.; resources, X.G., H.H. and F.T.; data curation, F.T.; writing—original draft preparation, B.L.; writing—review and editing, F.T.; visualization, J.Y.; supervision, F.T.; project administration, F.T.; funding acquisition, F.T., B.L., X.G. and H.H. All authors have read and agreed to the published version of the manuscript.

Funding: This research was funded by the National Key Research and Development Program of China (2018YFE0110000), the National Natural Science Foundation of China (11574258 and 11274259), the Scientific Research Starting Foundation Project of Fujian University of Technology (GY-Z220198), the Key Scientific and Technological Innovation Projects of Fujian Province (2022G02008), and the Education and Scientific Research Project of Fujian Provincial Department of Finance (GY-Z220232).

Institutional Review Board Statement: Not applicable.

Informed Consent Statement: Not applicable.

Data Availability Statement: The data presented in this paper are available after contacting the corresponding author.

Conflicts of Interest: The authors declare no conflict of interest.

References

1. Cypher, A.D.; Statscewich, H.; Campbell, R.; Danielson, S.L.; Eiler, J.; Bishop, M.A. Detection efficiency of an autonomous underwater glider carrying an integrated acoustic receiver for acoustically tagged Pacific herring. *ICES J. Mar. Sci.* **2023**, *80*, 329–341. [CrossRef]
2. Alaaeldeen, M.; Duan, W. Overview on the development of autonomous underwater vehicles (AUVs). *J. Ship Mech.* **2016**, *20*, 768–787.
3. Jiang, W.; Tao, Q.; Yao, J.; Tong, F.; Zhang, F. R&D of a low-complexity OFDM acoustic communication payload for Micro-AUV in confined space. *EURASIP J. Adv. Signal Process.* **2022**, *64*, 1–10. [CrossRef]
4. Jiang, W.; Yang, X.; Tong, F.; Yang, Y.; Zhou, T. A low-complexity underwater acoustic coherent communication system for small AUV. *Remote Sens.* **2022**, *14*, 3405. [CrossRef]
5. Huang, J.; Diamant, R. Adaptive modulation for long-range underwater acoustic communication. *IEEE Trans. Wirel. Commun.* **2020**, *19*, 6844–6857. [CrossRef]
6. Li, J.; Bai, Y.; Zhang, Y.; Qu, F.; Wei, Y.; Wang, J. Cross power spectral density based beamforming for underwater acoustic communications. *Ocean Eng.* **2020**, *216*, 107786. [CrossRef]
7. Cao, X.; Jiang, W.; Tong, F. Time reversal MFSK acoustic communication in underwater channel with large multipath spread. *Ocean Eng.* **2018**, *152*, 203–209. [CrossRef]
8. Jing, L.; Zhang, N.; He, C.; Shang, J.; Liu, X.; Yin, H. OTFS underwater acoustic communications based on passive time reversal. *Appl. Acoust.* **2022**, *185*, 108386. [CrossRef]
9. Fang, T.; Liu, S.; Ma, L.; Zhang, L.; Khan, I.U. Subcarrier modulation identification of underwater acoustic OFDM based on block expectation maximization and likelihood. *Appl. Acoust.* **2021**, *173*, 107654. [CrossRef]
10. Cai, J.; Li, Z.; Hao, Y.; Cai, J. Time-variant Doppler frequency estimation and compensation for mobile OFDM systems. *IEEE Trans. Consumer Electron.* **2006**, *52*, 336–340. [CrossRef]
11. Susaki, H. Method of high-resolution frequency measurement for pulse-Doppler sonar. In Proceedings of the 2002 International Symposium on Underwater Technology, Tokyo, Japan, 19 April 2002; pp. 39–44. [CrossRef]
12. Zhang, X.; Han, X.; Yin, J.; Sheng, X. Study on Doppler effects estimate in underwater acoustic communication. *J. Acoust. Soc. Am.* **2013**, *19*, 070062. [CrossRef]
13. Aval, Y.M.; Stohanovic, M. Partial FFT demodulation for coherent detection of OFDM signals over underwater acoustic communication. In Proceedings of the IEEE OCEANS, Bergen, Norway, 10–14 June 2013; pp. 1–4. [CrossRef]
14. Huang, Y.; Li, Y. Inter-carrier interference mitigation for differentially coherent detection in underwater acoustic OFDM system. In Proceedings of the IEEE International Conference on Communications, Montreal, QC, Canada, 14–23 June 2021; pp. 1–6. [CrossRef]
15. Yao, T.; Zhao, W.; Zhang, Q.; Kou, Y. Estimation of Doppler-shift based on correlation-peak waveform. In Proceedings of the International Conference on Communications, Circuits and Systems, Kokura, Japan, 11–13 July 2007; pp. 99–102. [CrossRef]
16. Li, B.; Tong, F.; Li, J.; Zheng, S. Cross-correlation quasi-gradient Doppler estimation for underwater acoustic OFDM mobile communications. *Appl. Acoust.* **2022**, *190*, 108640. [CrossRef]
17. Zakharov, Y.V.; Morozov, A.K. OFDM transmission without guard interval in fast-varying underwater acoustic channels. *IEEE J. Ocean. Eng.* **2015**, *40*, 144–158. [CrossRef]
18. Kay, S.M.; Doyle, S.B. Rapid estimation of the range-doppler scattering function. *IEEE Trans. Signal Process.* **2003**, *51*, 255–268. [CrossRef]
19. Abdelkareem, A.E.; Sharif, B.S.; Tsimenidis, C.C. Adaptive time varying doppler shift compensation algorithm for OFDM-based underwater acoustic communication systems. *Ad Hoc Netw.* **2016**, *45*, 104–119. [CrossRef]
20. Li, J.; Zakharov, Y.V.; Henson, B. Multibranch autocorrelation method for Doppler estimation in underwater acoustic channels. *IEEE J. Ocean. Eng.* **2018**, *43*, 1099–1113. [CrossRef]
21. Li, B.; Zheng, S.; Tong, F. Bit-error rate based Doppler estimation for shallow water acoustic OFDM communication. *Ocean Eng.* **2019**, *182*, 203–210. [CrossRef]
22. Li, B.; Tong, F.; Zheng, S.; Chen, D. Bit-error rate gradient descent Doppler estimation for underwater acoustic OFDM communication. *Appl. Acoust.* **2021**, *171*, 107557. [CrossRef]
23. Sharif, B.S.; Neasham, J.; Hinton, O.R.; Adams, A.E. A computationally efficient Doppler compensation system for underwater acoustic communications. *IEEE J. Ocean. Eng.* **2000**, *25*, 52–61. [CrossRef]
24. Zheng, S.; Tong, F.; Li, B.; Tao, Q.; Song, A.; Zhang, F. Design and evaluation of an acoustic modem for a small autonomous unmanned vehicle. *Sensors* **2019**, *19*, 2923. [CrossRef]
25. Haas, E.; Kaiser, S. Two-dimensional differential demodulation for OFDM. *IEEE Trans. Commun.* **2003**, *51*, 580–586. [CrossRef]
26. Stojanovic, M. Retrofocusing techniques for high rate acoustic communications. *J. Acoust. Soc. Am.* **2005**, *117*, 1173–1185. [CrossRef]